MITSUBISHI ELECTRIC RESEARCH LABORATORIES
http://www.merl.com

GaN HEMTs with Multi-functional p-Diamond Back-barriers

Zhang, Y.; Teo, K.H.; Palacios, T.

TR2016-069 June 2016

Abstract

This work for the first time explores the use of p-diamond as multi-functional back-barriers in GaN high electron mobility transistors (HEMTs). A well-calibrated self-consistent electro-thermal simulation has revealed that multi-functional p-diamond back-barriers can improve the performance of HEMTs, by achieving over 3 times higher breakdown voltage (BV), at least 30% higher thermal performance, enhanced 2DEG confinement and reduced short channel effects. These results indicate the great potential of the integration of GaN and diamond electronics for high-power and high-frequency applications.

IEEE International Symposium on Power Semiconductor Devices (ISPSD)

GaN HEMTs with Multi-functional p-Diamond Back-barriers

Yuhao Zhang, Tomás Palacios
Dept. of Electrical Engineering & Computer Science
Massachusetts Institute of Technology
Cambridge, MA, USA
yhzhang@mit.edu, tpalacios@mit.edu

Koon Hoo Teo
Mitsubishi Electric Research Laboratories
Cambridge, MA, USA
teo@merl.com

***Abstract*—This work for the first time explores the use of p-diamond as multi-functional back-barriers in GaN high electron mobility transistors (HEMTs). A well-calibrated self-consistent electro-thermal simulation has revealed that multi-functional p-diamond back-barriers can improve the performance of HEMTs, by achieving over 3 times higher breakdown voltage (*BV*), at least 30% higher thermal performance, enhanced 2DEG confinement and reduced short channel effects. These results indicate the great potential of the integration of GaN and diamond electronics for high-power and high-frequency applications.**

Keywords—p-type diamond; GaN HEMTs; back-barriers, power electronics

I. INTRODUCTION

GAN-based transistors and diodes are excellent candidates for high-voltage and high-frequency electronics. In particular, GaN high electron mobility transistors (HEMTs), which utilize a two-dimensional-electron-gas (2DEG) channel, have demonstrated excellent power and frequency performances [1]. However, applications such as radars for air traffic controller, satellites for broadcasting and high-power motors require an even higher power (~kW) at high-frequency (e.g. K-band), which are extremely challenging for GaN HEMTs to realize.

A promising method to further enhance the performances of GaN HEMTs is to incorporate diamond into GaN-based devices. As shown in Table I, diamond has ~3 times higher critical electric field (E_c) and ~10 times higher thermal conductivity than GaN. In addition, there is another complementary property of diamond to GaN electronics: p-type doping in diamond can be well realized with a doping concentration as high as 10^{18}-10^{21} cm^{-3} [2] , fee hole concentration over 10^{20} cm^{-3} [3] and a hole mobility of 300-600 cm^2/Vs [2]. In contrast, the p-doping in GaN has a maximum hole concentration of 10^{17}-10^{18} cm^{-3} and maximum hole mobility still below 30 cm^2/Vs [4][5].

Recent progress in GaN and diamond growth has made the integration of diamond and GaN devices possible. GaN layers can be epitaxially grown on [6] or wafer-transferred [7][8] to single-crystal [6] or polycrystalline [7][8] diamond substrates grown by chemical vapor deposition (CVD). Deposition of nanocrystalline diamond (NCD) coating has also been enabled to passivate GaN devices [9]. However, almost all current diamond and GaN integration merely focus on thermal management, which cannot take full advantage of the complementary properties of GaN and diamond.

In this work, we propose to incorporate diamond, as a multifunctional back-barrier, into GaN-based power and microwave devices for the first time. Electro-thermal simulation has demonstrated p-diamond capability in enhancing breakdown voltage, thermal performance and 2DEG confinement for GaN HEMTs.

TABLE I
MATERIAL PROPERTIES OF MAJOR SEMICONDUCTORS CONSIDERED FOR POWER AND MICROWAVE APPLICATIONS

	Si	GaAs	SiC	GaN	Diamond
E_g (eV)	1.1	1.4	3.3	3.4	5.5
μ_e (cm^2/Vs)	1400	8000	1000	2000	2000-4500
μ_h (cm^2/Vs)	600	400	100	850	3000-4000
E_c (MV/cm)	0.3	0.4	2.5	3.3	10
k_T (W/cmK)	1.3	0.46	4.2	1.3-2	10-20
ε	11.8	12.9	9.7	9	5.5

E_g: bandgap; μ_e, μ_h: electron and hole mobility; E_c: critical electric field; k_T: thermal conductivity; ε: dielectric constant. μ_e of 2DEG used for GaN.

II. SCHEMATIC STRUCTURE AND SIMULATION MODELS

The schematic of the GaN-on-diamond HEMT with a p-

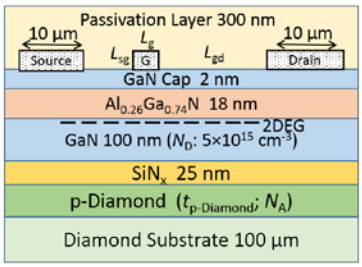

Power Device: L_{sg}=1.5 μm; L_g=2 μm; L_{gd}=10 μm
Microwave Device: L_{sg}=0.2 μm; L_g+ L_{gd}=1.7 μm; L_g=50-200 nm

Fig. 1. Schematic structure of a GaN-on-diamond HEMT with a p-diamond back-barrier. Two sets of source-to-gate distance (L_{sg}), gate length (L_g) and gate-to-drain distance (L_{gd}) are selected to simulate power and microwave devices.

This work is sponsored by Mitsubishi Electric Research Laboratories.

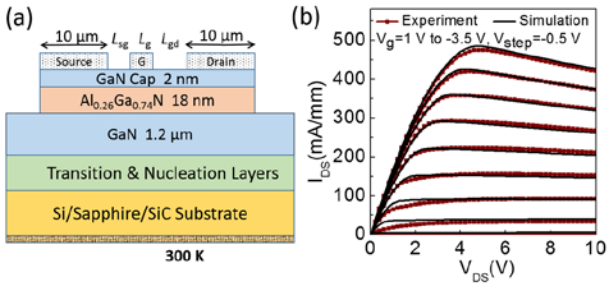

Fig. 2. (a) Schematic of the fabricated AlGaN/GaN HEMT structures on Si/Sapphire/SiC substrates that were used for simulation model calibration. (b) Comparison between simulation and experimental dc output characteristics for a single-finger GaN-on-Si HEMT.

diamond back-barrier is shown in Fig. 1. The AlGaN/GaN HEMT layers are based on the GaN-on-Si HEMTs fabricated at MIT [10][11]. The 2DEG density was revealed by Hall measurement as 1.25×10^{13} cm^{-2}. The GaN-on-diamond wafer structure is based on the experimental demonstration reported in [7][8], where the GaN layers would be extracted from epitaxial GaN-on-Si wafers, followed by the CVD growth of p-diamond back-barrier and 100 μm diamond substrate on top of a ~25 nm intermediate SiN_x dielectric layer. The p-diamond back-barrier thickness and doping concentration are denoted as $t_{p\text{-Diamond}}$ and N_A, respectively.

The self-consistent electro-thermal simulations were performed using the Silvaco ATLAS simulator, based on the models previously developed for GaN HEMTs at MIT [10]. The thermal conductivity of GaN and CVD-grown polycrystalline diamond was set as 1.8 W/cm·K and 15 W/cm·K [7], with a temperature dependence model described in [10]. Both NCD (10 W/cm·K [12]) and SiN_x (0.2 W/cm·K) are considered for device passivation. An effective thermal conductivity of 0.01 W/cm·K for SiN_x transitional dielectrics was calculated from the reported thermal boundary resistance in GaN-on-diamond structures [7]. The simulation models were calibrated by utilizing the fabricated HEMTs on Si substrates (Fig. 2).

III. HEMTs Performance Enhancements

A. Breakdown Voltage Enhancement

The insertion of p-diamond back-barrier can enhance device breakdown voltage (BV) by forming a reduced surface field (RESURF) structure. The p-diamond/n-GaN junction below the 2DEG channel can deplete the channel by a vertical electric field (E-field) at off-state, and thus spread the horizontal E-field. As shown in Fig. 3, the p-diamond/n-GaN junction greatly reduces the E-field peak at the gate edge and enables an almost uniform E-field distribution in GaN and diamond between gate and drain.

The RESURF design principle for HEMTs is to completely deplete the 2DEG charge by the p-n junction at breakdown. Dependence of device BV on p-diamond thickness t and acceptor (N_A) concentration was studied. As shown in Fig. 4, a maximum BV of ~1.9 kV can be achieved, which is more than

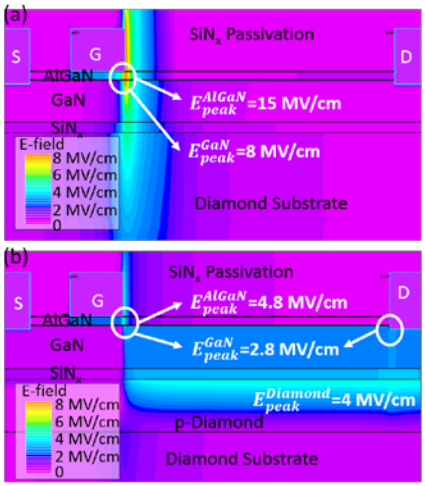

Fig. 3. Simulated electric field distribution in GaN-on-diamond HEMTs (a) without and (b) with a p-diamond back-barrier, both at an off-state bias of V_{GS}=-5 V and V_{DS}=1250 V.

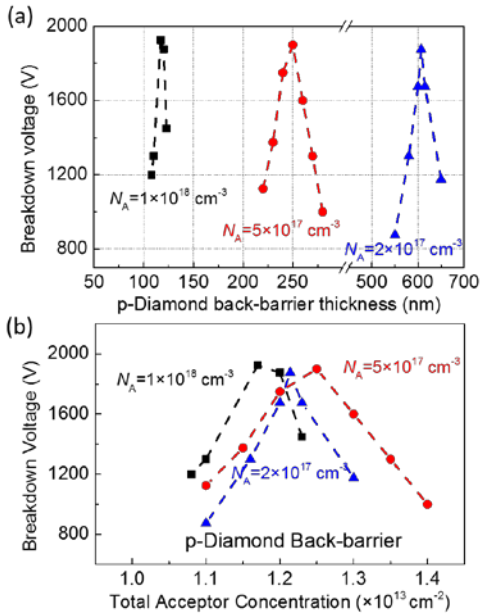

Fig. 4. (a) Breakdown voltage dependence on p-diamond back-barrier thickness at three different p-diamond doping levels; (b) Breakdown voltage dependence on total acceptor concentration for p-diamond back-barrier with different doping levels and thickness.

3 times of the BV of standard HEMTs (~500 V) (all with L_{gd}=10 μm). In addition, the high BV can be achieved by different N_A, with different optimized t correspondingly. All these optimized N_A and t correspond to the similar total charge density ($N_A \cdot t$) equivalent to the 2DEG density, showing the strong charge balance effect for complete depletion. This charge balance relationship has provided a great flexibility in selecting N_A and its corresponding optimized t for experimental demonstration.

B. Thermal Performance Enhancement

From the simulated lattice temperature distribution shown in Fig. 5, it can seen that the peak temperature T_{peak} locates at

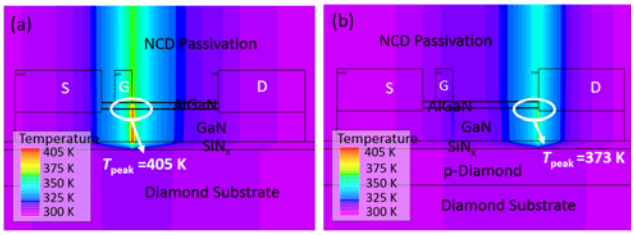

Fig. 5. Simulated lattice temperature distribution in GaN-on-diamond HEMTs (a) without and (b) with a p-diamond back-barrier, at a bias of V_{GS}=0 V and V_{DS}=30 V. The peak temperature and its location are denoted.

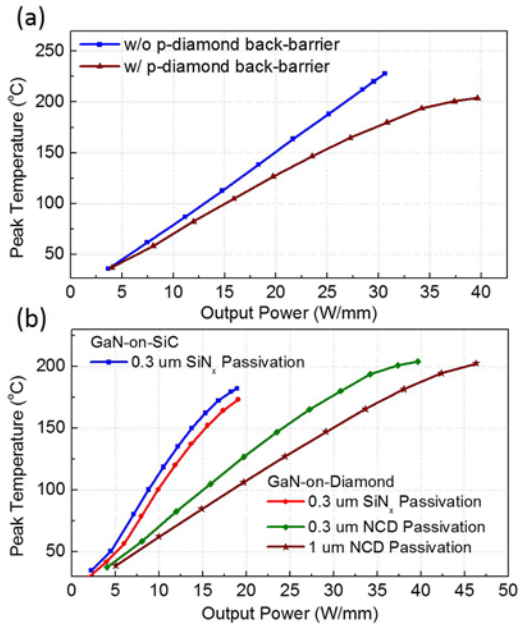

Fig. 6. Simulated peak temperature dependence on output power density for (a) GaN-on-diamond HEMTs with and without a p-diamond back-barrier. (b) GaN-on-SiC HEMTs with 0.3 µm SiN_x passivaiton, and GaN-on-diamond HEMTs with 0.3 µm SiN_x, 0.3 µm NCD and 1 µm NCD passivation on top of device.

the gate edge in standard GaN HEMTs and at the drain edge in GaN HEMTs with a p-diamond back-barrier, are the result of the combination of high E-field and high current density [10] at each location. In addition, a lower T_{peak} is observed in GaN HEMTs with a p-diamond back-barrier at the same bias, due to the E-field relaxation by p-diamond back-barrier.

Power *v.s.* T_{peak} dependence was simulated to present and compare device thermal performance [10], as the device peak temperature limit (e.g. 150 °C or 200 °C) determines the device maximumm allowable power dissipation. As shown in Fig. 6 (a), ~23% higher power density can be achieved in GaN HEMTs with p-diamond back-barriers compared to standard GaN-on-diamond HEMTs.

The influence of the layer structure on the thermal performance was also studied. As shown in Fig. 6 (b), for T_{peak}=150 °C, although the thermal conducvity of polycrystalline diamond is almost 4 times that of SiC, only ~15% higher power density was achieved in GaN-on-diamond than GaN-on-SiC. This is due to the large thermal boundary resistance of the intermediate dielectric layer used between diamond and GaN. However, if the surface passivation

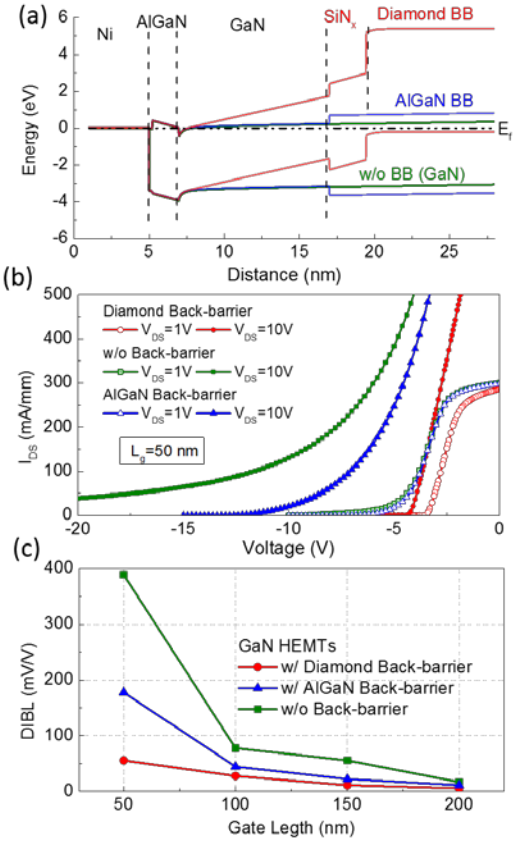

Fig. 8. Simulated (a) band-diagram and (b) transfer characteristics of GaN HEMTs without back-barrier (BB), with a p-diamond BB and with a AlGaN BB. (c) calculated DIBL of the three devices for the gate length of 50, 100, 150 and 200 nm. All the device simulated in this section utilized L_{sg}, L_g and L_{gd} of the "microwave device" illustrated in Fig. 1.

material changes from 0.3 µm SiN_x to 0.3 µm NCD, a ~50% power density increase can be achieved. If the thickness of NCD passivaiton increases from 0.3 µm to 1 µm, a power density over 30 W/mm, more than two times that of GaN-on-SiC, can be achieved for T_{peak}=150 °C. These results illustrate the great potential of NCD passivation in the thermal management of GaN power devices.

C. High-frequency Performance Enhancement

In GaN-based microwave devices, the gate length is typically scaled down below 200 nm. The short gate length causes short-channel effects such as threshold-voltage (V_{th}) shift, soft pinchoff and high sub-threshold current. A back-barrier structure with high bandgap (e.g. AlGaN [13]) or large polarizaiton charges (e.g. InGaN [14]) has been proposed to reduce short-channel effects and enhance 2DEG confinement.

P-diamond back-barrier can also form a large potential barrier that opposes the movement of electrons from 2DEG towards buffer layers, as shown in the simulated band diagram (Fig. 7 (a)). Thanks to the larger bandgap of diamond than GaN and the p-doping, p-diamond can form a larger energy barrier compared to conventional AlGaN back-barrier, and will induce a much smaller V_{th} shift and a significant improvement in the subthreshold slope (Fig. 7 (b)). The

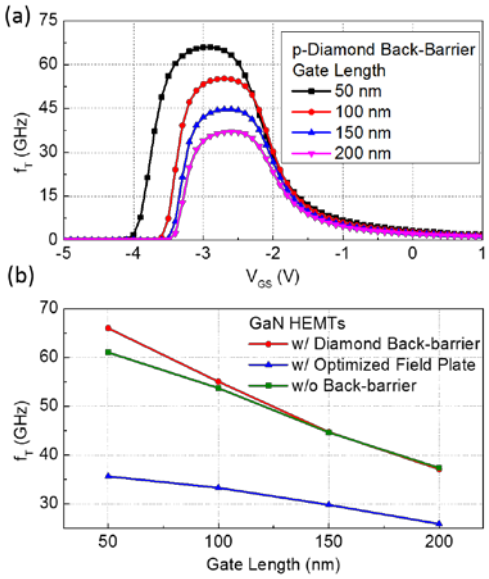

Fig. 9: (a) Simulated cut-off frequency f_T as a function of V_{gs} for GaN HEMTs with p-diamond back-barrier with 50, 100, 150 and 200 nm gate lengths. (b) Simulated peak cut-off frequency f_T of GaN-on-diamond HEMTs with and without p-diamond BB and with an optimized field plate structure. The AC simulation was conducted at f=1 MHz. All the device simulated in this section utilized L_{sg}, L_g and L_{gd} of the "microwave device" in Fig. 1.

enhanced suppresion of V_{th} shift by p-diamond back-barrier is more remarkable for shorter gate and higher frequencey devices, as shown in the simulated DIBL (defined as $\Delta V_{th}/\Delta V_{DS}$, and V_{DS} of 1 V and 10 V used in our simulation) as a function of gate length for GaN HEMTs with different back-barriers (Fig. 7 (c)).

Device transfer characteristics were then simulated in ac mode and transconductance g_m, gate capacitances C_{gd} and C_{gs} were extracted as a function of V_{GS}. The intrinsic cut-off frequency f_T was calculated by $f_T = \frac{g_m}{2\pi(C_{gs}+C_{gd})}$ for each V_{GS} and the peak f_T was extracted (Fig. 8 (a)). As shown in Fig. 8 (b), a slightly higher f_T is observed in GaN HEMTs with p-diamond back-barriers. To further compare the BV~f_T trade-off for microwave devices, HEMTs with a gate field plate (FP) are also simulated, as FP is a widely-used method to increase BV. The FP geometry was optimized according to [16]. The FP increases the BV from ~100 V to ~250 V (L_{sg}, L_g and L_{gd} shown in Fig. 1 for 'microwave device'), but introduces additional gate capacitance [16] and greatly reduces the device f_T (Fig. 8 (b)). In contrast, GaN HEMTs with a p-diamond back-barrier, with a ~400 V BV and >60 GHz f_T, outperforms the HEMTs with and without a FP in both BV and f_T.

IV. Conclution

In this work, we propose to insert p-diamond back-barriers into AlGaN/GaN HEMTs. This new structure take advantage of the complementary electrical properties of diamond and GaN, and is based on recent progress in GaN-on-diamond growth technologies. Electro-thermal simulations have demonstrated a large enhancement in the BV, thermal performance, 2DEG confinement and a reduction of short-channel effects. These results show the multiple functions of p-diamond back-barriers in the GaN HEMTs for high-power and high-frequency applications.

References

[1] R. S. Pengelly, S. M. Wood, J. W. Milligan, S. T. Sheppard, and W. L. Pribble, "A Review of GaN on SiC High Electron-Mobility Power Transistors and MMICs," *IEEE Trans. Microw. Theory Tech.*, vol. 60, no. 6, pp. 1764–1783, Jun. 2012.

[2] R. Kalish, "Doping of diamond," *Carbon*, vol. 37, no. 5, pp. 781–785, 1999.

[3] M. Werner, R. Job, A. Zaitzev, W. R. Fahrner, W. Seifert, C. Johnston, and P. R. Chalker, "The Relationship between Resistivity and Boron Doping Concentration of Single and Polycrystalline Diamond," *Phys. Status Solidi A*, vol. 154, no. 1, pp. 385–393, Mar. 1996.

[4] U. Kaufmann, P. Schlotter, H. Obloh, K. Köhler, and M. Maier, "Hole conductivity and compensation in epitaxial GaN: Mg layers," *Phys. Rev. B*, vol. 62, no. 16, p. 10867, 2000.

[5] I. P. Smorchkova, E. Haus, B. Heying, P. Kozodoy, P. Fini, J. P. Ibbetson, S. Keller, S. P. DenBaars, J. S. Speck, and U. K. Mishra, "Mg doping of GaN layers grown by plasma-assisted molecular-beam epitaxy," *Appl. Phys. Lett.*, vol. 76, no. 6, pp. 718–720, Feb. 2000.

[6] K. Hirama, M. Kasu, and Y. Taniyasu, "RF High-Power Operation of AlGaN/GaN HEMTs Epitaxially Grown on Diamond," *IEEE Electron Device Lett.*, vol. 33, no. 4, pp. 513–515, Apr. 2012.

[7] J. Pomeroy, M. Bernardoni, A. Sarua, A. Manoi, D. C. Dumka, D. M. Fanning, and M. Kuball, "Achieving the Best Thermal Performance for GaN-on-Diamond," in *2013 IEEE Compound Semiconductor Integrated Circuit Symposium (CSICS)*, 2013, pp. 1–4.

[8] D. C. Dumka, T. M. Chou, J. L. Jimenez, D. M. Fanning, D. Francis, F. Faili, F. Ejeckam, M. Bernardoni, J. W. Pomeroy, and M. Kuball, "Electrical and Thermal Performance of AlGaN/GaN HEMTs on Diamond Substrate for RF Applications," in *2013 IEEE Compound Semiconductor Integrated Circuit Symposium (CSICS)*, 2013, pp. 1–4.

[9] D. J. Meyer, T. I. Feygelson, T. J. Anderson, J. A. Roussos, M. J. Tadjer, B. P. Downey, D. S. Katzer, B. B. Pate, M. G. Ancona, A. D. Koehler, K. D. Hobart, and C. R. Eddy, "Large-Signal RF Performance of Nanocrystalline Diamond Coated AlGaN/GaN High Electron Mobility Transistors," *IEEE Electron Device Lett.*, vol. 35, no. 10, pp. 1013–1015, Oct. 2014.

[10] Y. Zhang, M. Sun, Z. Liu, D. Piedra, H. S. Lee, F. Gao, T. Fujishima, and T. Palacios, "Electrothermal Simulation and Thermal Performance Study of GaN Vertical and Lateral Power Transistors," *IEEE Trans. Electron Devices*, vol. 60, no. 7, pp. 2224–2230, Jul. 2013.

[11] Y. Zhang, M. Sun, S. J. Joglekar, T. Fujishima, and T. Palacios, "Threshold voltage control by gate oxide thickness in fluorinated GaN metal-oxide-semiconductor high-electron-mobility transistors," *Appl. Phys. Lett.*, vol. 103, no. 3, p. 033524, Jul. 2013.

[12] A. Wang, M. J. Tadjer, and F. Calle, "Simulation of thermal management in AlGaN/GaN HEMTs with integrated diamond heat spreaders," *Semicond. Sci. Technol.*, vol. 28, no. 5, p. 055010, 2013.

[13] D. S. Lee, X. Gao, S. Guo, and T. Palacios, "InAlN/GaN HEMTs With AlGaN Back Barriers," *IEEE Electron Device Lett.*, vol. 32, no. 5, pp. 617–619, May 2011.

[14] T. Palacios, A. Chakraborty, S. Heikman, S. Keller, S. P. DenBaars, and U. K. Mishra, "AlGaN/GaN high electron mobility transistors with InGaN back-barriers," *IEEE Electron Device Lett.*, vol. 27, no. 1, pp. 13–15, Jan. 2006.

[15] S. Adak, A. Sarkar, S. Swain, H. Pardeshi, S. K. Pati, and C. K. Sarkar, "High performance AlInN/AlN/GaN p-GaN back barrier Gate-Recessed Enhancement-Mode HEMT," *Superlattices Microstruct.*, vol. 75, pp. 347–357, Nov. 2014.

[16] S. Karmalkar and U. K. Mishra, "Enhancement of breakdown voltage in AlGaN/GaN high electron mobility transistors using a field plate," *IEEE Trans. Electron Devices*, vol. 48, no. 8, pp. 1515–1521, Aug. 2001.